

# Collective Edge Excitations In The Quantum Hall Regime: Edge Helicons And Landau-level Structure

O. G. Balev\* and P. Vasilopoulos†

\*Institute of Physics of Semiconductors, National Academy of Sciences, 45 Prospekt Nauky, Kiev 252650, Ukraine

†Concordia University, Department of Physics, 1455 de Maisonneuve Blvd O, Montréal, Québec, Canada, H3G 1M8

Based on a *microscopic* evaluation of the local current density, a treatment of edge magnetoplasmons (EMP) is presented for confining potentials that allow Landau level (LL) flattening to be neglected. Mode damping due to electron-phonon interaction is evaluated. For  $\nu = 1, 2$  there exist independent modes spatially *symmetric* or *antisymmetric* with respect to the edge. Certain modes, changing shape during propagation, are nearly undamped even for very strong dissipation and are termed **edge helicons**. For  $\nu > 2$  inter-LL Coulomb coupling leads to a strong repulsion of the **decoupled** LL fundamental modes. The theory agrees well with recent experiments.

PACS numbers:

The essentially classical treatments [1]- [2] of low-frequency collective excitations, propagating along the edges of a two-dimensional electron gas (2DEG) subject to a normal magnetic field  $B$ , termed in Ref. [3] edge magnetoplasmons (EMP), account for some important characteristics of EMP, e.g., the gapless spectrum of these excitations [1] and the *acoustic* modes [2], [4]. However, the results of Refs. [1] and [2] are valid, respectively, for infinitely sharp and smooth density profiles that are independent of the filling factor  $\nu$ . As contrasted in Fig. 1 with our calculated density profile for one or two LLs occupied and a smooth , on the magnetic length  $\ell_0 = \sqrt{\hbar}/|e|B$  scale, parabolic confining potential these assumed profiles miss an important quantum mechanical aspect, the LL structure. This inadequacy was manifested in the observed [4] plateau structure of the transit times reflecting that of the quantum Hall effect (QHE) plateaus and not accounted for in Ref. [2]. In addition, for a spatially homogeneous dissipation within the channel, the damping is found quantized and independent of temperature [1] or it is treated phenomenologically [2] with damping rates strongly overestimated [4]. Other limitations of the model of Ref. [1] were pointed out in Refs. [5]- [6]. In a sense the conventional EMPs [1]- [3] is the magnetic analog of the Kelvin wave [7] at the edge of a rotating "shallow" sea with chirality determined by the Coriolis parameter which corresponds to the cyclotron frequency  $\omega_c = |e|B/m^*$ . In these mostly *classical* models the position of the edge does not vary but the charge density profile at the edge does.

In another distinctly different and fully quantum-mechanical edge wave mechanism [8-10] only the edge position, for  $\nu = 1$ , of an incompressible 2DEG varies; with respect to that the density profile is that of the undisturbed 2DEG. This approach is limited to the subspace of the lowest LL wave functions, neglects LL mixing and dissipation, and results in a single chiral EMP with dispersion law similar to that in [1].

Both previous classes of models are oversimplifications. In this Letter we present a quasi-microscopic treatment of EMPs for integer  $\nu$ , which takes into account LL struc-

ture, LL mixing, dissipation (related to LL mixing essentially), and the inhomogeneity of the current density near the edges treated recently [11]. It is valid for bare confining potentials sufficiently steep that LL flattening and the formation of compressible and incompressible strips [12] can be neglected [13]; in this case the dissipation is essential only within a distance  $\lesssim \ell_0$  from the edges [11]. As will be made clear, our model effectively incorporates the previous two distinct propagation mechanisms.

We consider a zero-thickness 2DEG, of width  $W$  and of length  $L_x = L$ , in the presence of a strong magnetic field  $B$  along the  $z$  axis. We take the confining potential flat ( $V_y = 0$ ) in the interior of the 2DEG and parabolic at its edges,  $V_y = m^*\Omega^2(y - y_r)^2/2$ ,  $y \geq y_r$ .  $V_y$  is assumed smooth on the scale of  $\ell_0$  such that  $\Omega \ll \omega_c$ . The resulting one-electron energy spectrum  $E_n(k_x) = (n + 1/2)\hbar\omega_c + m^*\Omega^2(y_0 - y_r)^2/2$ , where  $y_0 = \ell_0^2 k_x \geq y_r$ , leads to the group velocity of the edge states  $v_{gn} = \partial E_n(k_e^{(n)})/\hbar\partial k_x = \hbar\Omega^2 k_e^{(n)}/m^*\omega_c^2$  with characteristic wave vector  $k_e^{(n)} = (\omega_c/\hbar\Omega)\sqrt{2m^*\Delta_{Fn}}$ ,  $\Delta_{Fn} = E_F - (n + 1/2)\hbar\omega_c$ . The edge of the  $n$ -th LL is denoted by  $y_{rn} = y_r + \ell_0^2 k_e^{(n)}$  and  $W = 2y_{r0}$ .

Assuming  $|q_x|W \gg 1$ , we can consider an EMP along the right edge of the channel of the form  $A(\omega, q_x, y) \exp[-i(\omega t - q_x x)]$ , totally independent of the left edge. We neglect the spin-splitting for  $\nu$  even. Because the wavelength  $\lambda$  of the practically quasi-static EMP satisfies  $\lambda \gg \ell_0$ , the electric field  $E_x(\omega, q_x, y)$  has a smooth  $y$  dependence on the scale of  $\ell_0$ . Following Ref. [11] we obtain the current density  $j_\mu$  in the form  $j_y(y) = \sigma_{yy}(y)E_y(y) + \sigma_{yx}^0(y)E_x(y)$ ,  $j_x(y) = \sigma_{xx}(y)E_x(y) - \sigma_{yx}^0(y)E_y(y) + \sum_j v_{gj} \delta\rho_j(\omega, q_x, y)$ . The convection contribution  $v_{gj} \delta\rho_j$  is due to a charge distortion  $\delta\rho_j$  localized near the edge of the  $j$ -th LL. These contributions to  $j_\mu$  are microscopically obtained when  $E_\mu(y)$  is smooth on the scale of  $\ell_0$ . This holds for the components  $\propto E_x(y)$  but is not well justified for those  $\propto E_y(y)$ . We approximate the latter by those obtained when  $E_y(y)$  is smooth. This is equivalent to neglecting nonlocal contributions to  $j_\mu \propto \int dy' \sigma_{\mu y}(y, y') E_y(y')$ . For weak dissi-

pation the results for the fundamental modes can be justified by a *microscopic* RPA treatment [14] which includes nonlocal effects and does not require the smoothness of  $E_\mu(y)$  on the scale of  $\ell_0$ . The Hall conductivity

$$\sigma_{yx}^0(y) = \frac{e^2}{2\pi\hbar} \sum_n \int_{-\infty}^{\infty} dy_0 f(E_{nk_x}) \Psi_n^2(y - y_0), \quad (1)$$

where  $\Psi_n(y)$  is a harmonic oscillator function and  $f(E_{nk_x})$  the Fermi-Dirac function. We consider only the interaction of electrons with piezoelectric phonons and neglect that with impurities shown to be very weak [15]. We approximate  $\sigma_{xx}(y)$  by  $\sigma_{yy}(y) = \sum_n \sigma_{yy}^{(n)}(y)$  and calculate it for very low temperatures  $T \ll \hbar v_{gn}/\ell_0 k_B$  using Ref. [11]. For  $v_{gn} > s$  and  $\nu = 2, 4$  we obtain  $\sigma_{yy}^{(n)}(y) = \tilde{\sigma}_{yy}^{(n)} \Psi_n^2(\bar{y}_n)$ ,  $\bar{y}_n = y - y_{rn}$ , and  $\tilde{\sigma}_{yy}^{(n)} = 3e^2 \ell_0^4 c' k_B^3 T^3 / \pi^2 \hbar^6 v_{gn}^4 s$  where  $s$  is the speed of sound and  $c'$  the interaction constant.

Using  $j_\mu$ , the continuity equation linearized in  $\delta\rho \equiv \rho$ , and Poisson's equation we obtain the integral equation

$$\begin{aligned} -i \sum_n (\omega - q_x v_{gn}) \rho_n(\omega, q_x, y) + \frac{2}{\epsilon} \left[ q_x^2 \sigma_{xx}(y) \right. \\ \left. - i q_x \frac{d}{dy} [\sigma_{yx}^0(y)] - \sigma_{yy}(y) \frac{d^2}{dy^2} - \frac{d}{dy} [\sigma_{yy}(y)] \frac{d}{dy} \right] \\ \times \int_{-\infty}^{\infty} dy' K_0(|q_x||y - y'|) \rho(\omega, q_x, y') = 0, \quad (2) \end{aligned}$$

where  $\epsilon$  is the spatially homogeneous dielectric constant. For a dissipationless, classical 2D electron liquid Eq. (2) becomes identical with Eq. (4) of Ref. [2]. If  $\sigma_{\mu\nu}^0(y)$  is independent of  $y$ , for  $|y| < W/2$ , Eq. (2) reduces to Eq. (15) of Ref. [1]. To solve Eq. (2), we remark that for  $\hbar v_{gn} \gg \ell_0 k_B T$  we have  $d[\sigma_{yx}^0(y)]/dy \propto [\Psi_0^2(\bar{y}_0) + \Psi_1^2(\bar{y}_1)]$ . It follows that  $\rho_n(\omega, q_x, y)$  is concentrated within a region of extent  $\sim \ell_0$  around the edge of the  $n$ th LL. For  $2\Delta y = y_{r0} - y_{r1} \gg \ell_0$ , cf. Fig. 1, we neglect the exponentially small overlap between  $\rho_0(\omega, q_x, y)$  and  $\rho_1(\omega, q_x, y)$  and, for  $\nu = 4$ , attempt the exact solution

$$\begin{aligned} \rho(\omega, q_x, y) = \Psi_0^2(\bar{y}_0) \sum_{n=0}^{\infty} \rho_0^{(n)}(\omega, q_x) H_n(\bar{y}_0/\ell_0) \\ + \Psi_1^2(\bar{y}_1) \sum_{l=0}^{\infty} \rho_1^{(l)}(\omega, q_x) H_l(\bar{y}_1/\ell_0), \quad (3) \end{aligned}$$

where  $H_n(x)$  are the Hermite polynomials. We call the terms  $l = 0, 1, 2$ , etc., the monopole, dipole, quadrupole, etc. terms in this expansion of  $\rho_n(\omega, q_x, y)$ .

We now multiply Eq. (2) by  $H_m(\bar{y}_0/\ell_0)$  and integrate over  $y$ . This procedure is repeated with  $H_k(\bar{y}_1/\ell_0)$ . With the abbreviations  $\rho_0^{(m)}(\omega, q_x) \equiv \rho_0^{(m)}$ ,  $a_{mk}(q_x) \equiv a_{mk}$  etc., we obtain, the coupled systems of equations

$$\bar{\omega}_0 \rho_0^{(m)} - S_{0m} \sum_{n=0}^{\infty} c_{mn} [a_{mn} \rho_0^{(n)} + b_{mn} \rho_1^{(n)}] = 0, \quad (4)$$

$$\begin{aligned} \bar{\omega}_1 \left[ A_k \rho_1^{(k)} + B_k \rho_1^{(k+2)} + \rho_1^{(k-2)}/2 \right] / 2 \\ - \sum_{n=0}^{\infty} c_{kn} \left[ S_{1k} F_{nk}/2 - \sqrt{k} S_1 \tilde{F}_{nk} \right] = 0. \quad (5) \end{aligned}$$

Here  $\bar{\omega}_n = \omega - q_x v_{gn}$ ,  $F_{nm} = b_{nm} \rho_0^{(n)} + d_{mn} \rho_1^{(n)}$ ,  $\tilde{F}_{nm} = \tilde{b}_{nm} \rho_0^{(n)} + \tilde{d}_{mn}$ ,  $S_{nm} = S_n + m S'_n$ ,  $S_n = 2(q_x \sigma_{yx}^0 - i q_x^2 \tilde{\sigma}_{xx}^{(n)})/\epsilon$ ,  $S'_n = -4i \tilde{\sigma}_{yy}^{(n)}/\epsilon \ell_0^2$ , and  $\sigma_{yx}^0 = e^2/\pi\hbar$ .  $a_{mn}$  is given in Ref. [16] and  $b_{mn}$ ,  $\tilde{b}_{mn}$ ,  $d_{mn}$ , and  $\tilde{d}_{mn}$  are given by similar expressions. Further,  $c_{mn} = (2^n n! / 2^m m!)^{1/2}$ ,  $A_m = (2m + 1)$ , and  $B_m = (m + 2)(2m + 2)$ .

(i)  $\nu = 2$ . In this case the second term of Eq. (3), the third term of Eq. (4), and Eq. (5) are absent. Eqs. (3), (4), and the form of  $a_{mn}$  show [16] that there exist *independent* modes, spatially *symmetric*,  $\rho^s(\omega, q_x, y)$ , or *antisymmetric*,  $\rho^{as}(\omega, q_x, y)$ , with respect to  $y = y_{r0}$ ; they correspond to  $n$  *even* or *odd*, respectively.

*Symmetric modes.* We first consider only two terms,  $n = 0$  and  $n = 2$ , in Eq. (3). For  $m = 0$  and  $m = 2$  Eq. (4) gives a system of two coupled equations for the unknowns  $\rho_0^{(0)}$  and  $\rho_0^{(2)}$ . The vanishing of the determinant gives two branches  $\omega_+^s$  and  $\omega_-^s$ . With  $v_g \equiv v_{g0}$  and  $S \equiv S_0$  their dispersion relations (DRs) read [16]  $\omega_{\pm}^s = q_x v_{gn} + \{R_{\pm} \pm [R_{\pm}^2 + 4S(S + 2S')a_{02}^2]^{1/2}\}/2$ , where  $R_{\pm} = [S(a_{00} \pm a_{22}) \pm 2S' a_{22}]$ .

**Edge helicons.** The coupling between the branches (due to  $a_{02} \neq 0$ ) and the strength of the dissipation modify the character of the pure modes. For  $K \gg \eta$ ,  $\eta = \tilde{\sigma}_{yy}^{(0)}/\ell_0^2 \sigma_{yx}^0 |q_x|$ , and *weak dissipation*  $\eta < 1/4$ , the  $\omega_-^s$  branch remains almost unchanged whereas the  $\omega_+^s$  branch acquires a principally new contribution to damping since  $\omega_+^s = q_x v_g + S(K + 1/4) + S'/4K$ ,  $K = 1/2 - \ln(q_x \ell_0)$ . The coupling leaves the phase velocity of both branches nearly unchanged and the  $\omega_+^s$  branch is *very weakly damped* and almost monopole-like since  $\rho_0^{(0)}/\rho_0^{(2)} \approx -8K$ ,  $K \gg 1$ . For *strong dissipation* ( $K \gg \eta \gg 1/4$ ) we obtain  $\rho_0^{(0)}/\rho_0^{(2)} \approx -2iK/\eta$ . This corresponds to  $\omega_+^s \tau_0^* \gg \nu r_0/\pi \gg \omega_+^s \tau_0^*/(4K + 1)$ , where  $r_0 = e^2/\epsilon \hbar \omega_c \ell_0$ , and  $\omega_+^s$  can still be considered high compared to  $1/\tau_0^*$ ;  $\tau_n^*$ , defined by  $1/\tau_n^* = \omega_c \tilde{\sigma}_{yy}^{(n)}/(\sigma_{yx}^0 \ell_0 \sqrt{2n + 1})$ , is an effective scattering time in an edge strip of width  $\ell_0 \sqrt{2n + 1}$ . In this frequency region we call the  $\omega_+^s \equiv \omega_{EH}^{(0)}$  branch high-frequency *edge helicon* (HFEH). Due to the almost  $\pi/2$  shift between  $\rho_0^{(0)}$  and  $\rho_0^{(2)}$ , the HFEH exhibits the following remarkable property: if its charge along  $y$  has a pure quadrupole character  $\propto |\rho_0^{(2)}|$  for some phase of the wave, after approximately a  $\pm\pi/2$  shift it acquires a pure monopole character  $\propto |\rho_0^{(0)}|$ . Notice that  $\text{Im}\omega_{EH}^{(0)} \propto T^3$ . That is, in contrast with Ref. [1], the damping of the HFEH scales with  $T$  and is not quantized in the QHE plateaus. As for the  $\omega_-^s$  branch, it is strongly damped.

For *very strong dissipation*,  $\eta \gg K$ , the  $\omega_-^s$  branch is strongly damped while the  $\omega_+^s$  branch changes to a low-frequency *edge helicon* (LFEH) with DR ( $\omega_+^s \equiv \omega_{EH}^{LF}$ )

$$\omega_{EH}^{LF} = q_x v_g + [S - i\tilde{\sigma}_{yy}^{(0)}/\eta^2 \ell_0^2 \epsilon](K - 1/4), \quad (6)$$

where  $\omega_{EH}^{LF} \tau_0^* \ll \nu r_0/\pi \lesssim 1$ . Despite this, the LFEH is *very weakly damped*. Further,  $\rho_0^{(0)}/\rho_0^{(2)} \approx 2$  and Eq. (3) gives the charge density profile  $\delta\rho = \sqrt{\pi}\ell_0 \text{Re}[\rho(\omega, q_x, y)/\rho_0^{(0)}(\omega, q_x)]$  shown in Fig. 2 by curve 2 for  $K/\eta = 0.01$ ; such a small ratio has practically no effect on  $\delta\rho(y)$  if only the terms  $n = 0$  and  $n = 2$  are kept in Eq. (3). Since  $\delta\rho(y)$  is symmetric with respect to the edge, only one half of Fig. 2 is shown. Curve 1 shows the monopole term ( $\propto \Psi_0^2$ ). The effective convergence parameter for curve 2 is not sufficiently small. To better describe the profile of the LFEH we also plot curves 3, 4, and 5 obtained with 3, 4, and 5 even  $n$  terms retained in Eq. (3), respectively. As shown, keeping 4 or 5 terms in the  $n$ -summation leads already to a clear convergence in the form of the charge-density profile, without altering its oscillatory character or changing its magnitude by much. This oscillatory behavior of  $\delta\rho$ , further modified during propagation, is in sharp contrast with the “usual” EMPs of Ref. [1] and the  $j = 0$  mode of Ref. [2]. Equation (6) already approximates well  $\text{Re}\omega_{EH}^{LF}$  and the dependence of  $\text{Im}\omega_{EH}^{LF}$  on  $T$ .

The *antisymmetric* modes have been described in Ref. [16]. Here it is worth mentioning that if we keep only one, two, or three *odd* terms in Eq. (3), the dimensionless velocity of the dipole branch  $v_{dip} = (\omega/q_x - v_{g0})/(e^2/\pi\hbar\epsilon)$  for weak dissipation is equal, respectively, to 0.4996, 0.5963, and 0.6287; the charge density profile shows a similar fast convergence.

It is worth noticing that if we limit ourselves to the subspace of the  $n = 0$  LL wave functions, by keeping, for  $\nu = 1$ , only the  $n = 0$  term in Eq. (3), we have the same edge-wave mechanism as Refs. [8]- [10] with the same single mode. This can be seen by writing  $n(x, y, t) = n_0(y + b(\omega, q_x) \cos(\omega t - q_x x)) \approx n_0(y) + [dn_0(y)/dy]b(\omega, q_x) \cos(\omega t - q_x x)$ , with  $dn_0(y)/dy \sim \psi_0^2(\bar{y}_0)$ , for the total density  $n(x, y, t)$ . It is only by retaining the  $n \geq 1$  terms that we obtain more than one modes with important contributions to the damping of the fundamental mode. Further, retaining the  $n \geq 1$  terms is equivalent to incorporating in the model the classical edge-wave mechanism [1]- [3], [7]. It is also clear that we focus on wave effects of non-spin nature and do not treat spin excitations such as skyrmions.

**(ii) inter-LL coupling:**  $\nu = 4$ . Although the condition  $2\Delta y \gg \ell_0$ , cf. Fig. 1, is well justified for  $V_y$ , the system of Eqs. (4) and (5) can be strongly coupled due to the long-range nature of the Coulomb interaction. To make contact with the  $\nu = 2$  results, we first consider the *symmetric* modes,  $\rho_1^{(0)}$  and  $\rho_1^{(2)}$  of the  $n = 1$  LL **decoupled** from the  $n = 0$  LL. Then one branch is  $\omega_3^{(1)} \approx q_x v_{g1} + (S_1 + 2S_1^i)/4$ . The other one is the fundamental branch, or HFEH of the  $n = 1$  LL,  $\omega_{EH}^{(1)} \approx q_x v_{g1} + S_1(K - 1/4) + S_1^i/12K$ . Now the **decoupled** fundamental modes of  $n = 0$  and  $n = 1$  LLs have DRs given by  $\omega_{EH}^{(0)}$  and  $\omega_{EH}^{(1)}$ . When they are **coupled**, their DRs

change drastically. For  $2\Delta y \gg \ell_0$  and  $2\Delta y q_x \ll 1$  an examination of the coefficients  $a_{mn}$  etc. shows that the most important terms in Eq. (3) are  $\rho_0^{(0)}$ ,  $\rho_1^{(0)}$ , and  $\rho_1^{(2)}$ . This leads to three branches,  $\tilde{\omega}_{\pm}^{(01)}$  and  $\omega_3^{(01)} \approx \omega_3^{(1)}$ . The renormalized  $n = 0$  LL fundamental mode becomes  $\tilde{\omega}_+^{(01)} \approx q_x(v_{g0} + v_{g1})/2 + (2/\epsilon)q_x\sigma_{yx}^0 [2\ln(1/q_x\ell_0) - \ln(2\Delta y/\ell_0) + 3/5] + S_1^i/16K$  and that of the  $n = 1$  LL  $\omega_-^{(01)} \approx q_x(v_{g0} + v_{g1})/2 + (2/\epsilon)q_x\sigma_{yx}^0 [\ln(2\Delta y/\ell_0) + 2/5] + S_1^i/\{24[\ln(\Delta y/\ell_0) + \gamma + 1/4]\}$ , where  $\gamma$  is the Euler constant. The  $\omega_-^{(01)}$  mode becomes purely acoustic and has a phase velocity larger than that of the  $j = 1$  mode of Ref. [2] for  $2\Delta y/\ell_0 \geq 5$ . The coupled fundamental modes  $\tilde{\omega}_{\pm}^{(01)}$  are very weakly damped.

The DRs for  $\nu = 4$ , corresponding to the experimental [4] parameters  $B = 2.06$  Tesla and  $T = 1.5K$ , are shown in Fig. 3. The solid and short-dashed curves are obtained with  $\epsilon = 12.5$ . The dashed curves ( $\epsilon = 6.75$ ) pertain to a sample with air above the spacer. The short-dashed curves are the **decoupled** fundamental modes, the solid and dashed ones the **coupled** modes. As can be seen, the inter-LL coupling strongly modifies the DR of both fundamental modes. Using  $\Omega = 7.8 \times 10^{11}/\text{sec}$  [17] gives  $\Omega/\omega_c \approx 0.14$ ,  $2\Delta y/\ell_0 \approx 6$ ,  $v_{g0} = 2.3 \times 10^6/\text{sec}$ , and  $v_{g0}/v_{g1} = \sqrt{3}$ . The  $\nu = 4$  modes, in Fig. (3a) of Ref. [4], are very well described by the renormalized fundamental modes  $\tilde{\omega}_{\pm}^{(01)}$ . The same holds for the  $\nu = 4$  modes of Fig. 3 (b) of Ref. [4]. The mode  $\omega_3^{(01)}$  is strongly damped: with  $\epsilon = 6.75$  its decay rate is  $\text{Im}S_1^i/2 \approx 2\tilde{\sigma}_{yy}^{(1)}/\epsilon\ell_0^2 \approx 1.3 \times 10^{10}/\text{sec}$ . This is smaller than that of the  $j = 1$  branch of Ref. [2]  $1/\tau_1 \approx 2 \times 10^{10}/\text{sec}$ . The decay rate of the  $j = 0$  mode is  $1/\tau_0 \approx 1.7 \times 10^9/\text{sec}$  whereas those of the  $\tilde{\omega}_{\pm}^{(01)}$  modes are about ten times smaller,  $\text{Im}\tilde{\omega}_+^{(01)} \approx 2.1 \times 10^8/\text{sec}$  and  $\text{Im}\tilde{\omega}_-^{(01)} \approx 5.6 \times 10^8/\text{sec} \ll 1/\tau_1 \approx 2 \times 10^{10}/\text{sec}$ . Thus, the decay rates of the  $\tilde{\omega}_{\pm}^{(01)}$  modes should be much closer to those of the experiment [4] than the strongly overestimated ones [2]. Regarding the delay times  $t_d$  for the sample with length  $L_x = 320\mu\text{m}$ , we obtain  $t_d = 1.2 \times 10^{-10}\text{sec}$  for the  $\tilde{\omega}_+^{(01)}$  mode and  $t_d = 6.9 \times 10^{-10}\text{sec}$  for the  $\tilde{\omega}_-^{(01)}$  mode, in very good agreement with the observations [4]. We conclude that the slower mode observed for  $\nu = 4$  is not the  $j = 1$  mode of Ref. [2] but the present  $\tilde{\omega}_-^{(01)}$  mode. It is also clear that our theory accounts for the existence of the plateaus in  $t_d$  [4] as the quantized Hall conductivity appears in all DRs.

In summary, we presented a theory of edge magnetoplasmons for confining potentials that allow LL flattening to be neglected. It accounts for the existence of plateaus in the delay times, the dispersion relations, and the damping rates of the observed [4] modes for  $\nu = 4$ . Compared to the *decoupled*, individual LL fundamental modes, the **coupled** LL modes are drastically renormalized and in good agreement with the experiment. Other novel results are mentioned in the abstract.

This work was supported by NSERC Grant No.

- 
- [1] V. A. Volkov and S. A. Mikhailov, Zh. Eksp. Teor. Fiz. **94**, 217 (1988) [Sov. Phys. JETP **67**, 1639 (1988)] .
  - [2] I. L. Aleiner and L. I. Glazman, Phys. Rev. Lett. **72**, 2935 (1994).
  - [3] D. B. Mast *et al.*, Phys. Rev. Lett. **54**, 1706 (1985); D. C. Glatti *et al.*, *ibid* **54**, 1710 (1985).
  - [4] G. Ernst *et al.*, Phys. Rev. Lett. **77**, 4245 (1996).
  - [5] V. I. Tal'yanskii *et al.*, Surf, Sci. **229**, 40 (1990).
  - [6] R. C. Ashoori *et al.*, Phys. Rev. B **45**, 3894 (1992).
  - [7] Kelvin, William Thomson, Phil. Mag. **x**, 97 (1880).
  - [8] X. G. Wen, Phys. Rev. B **43**, 11025 (1991); M. Stone, Ann. Phys. (NY) **207**, 38 (1991).
  - [9] J. S. Giovanazzi *et al.*, Phys. Rev. Lett. **72**, 3230 (1994); J. J. Palacios and A. H. MacDonald, *ibid* **76**, 118 (1996).
  - [10] M. Stone *et al.*, Phys. Rev. B **45**, 14156 (1992); C. de Chamon and X. G. Wen, *ibid* **49**, 8227 (1994); U. Zulicke and A. H. MacDonald, *ibid* **54**, 16813 (1996).
  - [11] O. G. Balev and P. Vasilopoulos, Phys. Rev. B **54**, 4863 (1996).
  - [12] D. B. Chklovskii *et al.*, Phys. Rev. B **46**, 4026 (1992).
  - [13] L. Brey *et al.*, Phys. Rev. B **47**, 13884 (1993).
  - [14] O. G. Balev and P. Vasilopoulos, to be published.
  - [15] J. H. Han and D. J. Thouless, Phys. Rev. B **55**, R1926 (1997).
  - [16] O. G. Balev and P. Vasilopoulos, Phys. Rev. B **56**, 13252 (1997).
  - [17] G. Muller *et al.*, Phys. Rev. B **45**, 3932 (1992).

FIG. 1. Unperturbed electron density  $n_0(y)$ , normalized to the bulk value  $n_0$ , as a function of  $y/\ell_0$ . The thick solid curve is the model of Ref. [1] and the short-dashed curve that of Ref. [2] ( $a/\ell_0 = 20$ ). The dashed and solid curves show the calculated profile for  $\nu = 1, 2$  and for  $\nu = 4$ , respectively. The solid and open dots mark the edges of the  $n = 1$  and  $n = 0$  LLs.

FIG. 2. Dimensionless charge density profile  $\tilde{\rho}(y)$  of the low-frequency edge helicon as a function of  $\tilde{y}_0/\ell_0$  for  $\nu = 2$ . The number of *even* terms retained in Eq. (3) is shown next to the curves.

FIG. 3. EMP dispersion relations pertinent to Ref. [4] for  $\nu = 4$ . The short-dashed curves are the **decoupled** fundamental modes ( $\epsilon = 12.5$ ). The upper two solid ( $\epsilon = 12.5$ ) and dashed ( $\epsilon = 6.75$ ) curves are the **coupled** fundamental modes. The lowest solid (dashed) curve is the third branch  $\omega_3^{(01)} \approx \omega_3^{(1)}$ . The accessible [4] frequencies are below  $\omega = 0.01\omega_c$ .

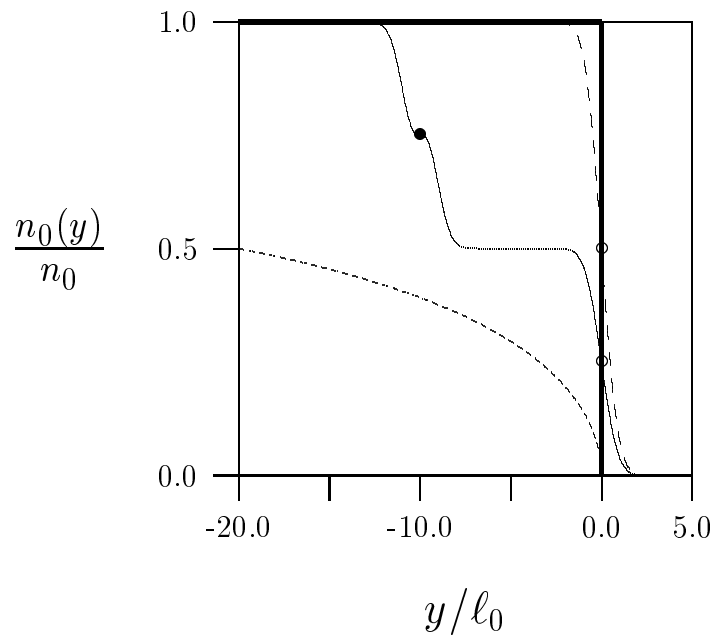


Fig. 1, Balev *et al.*

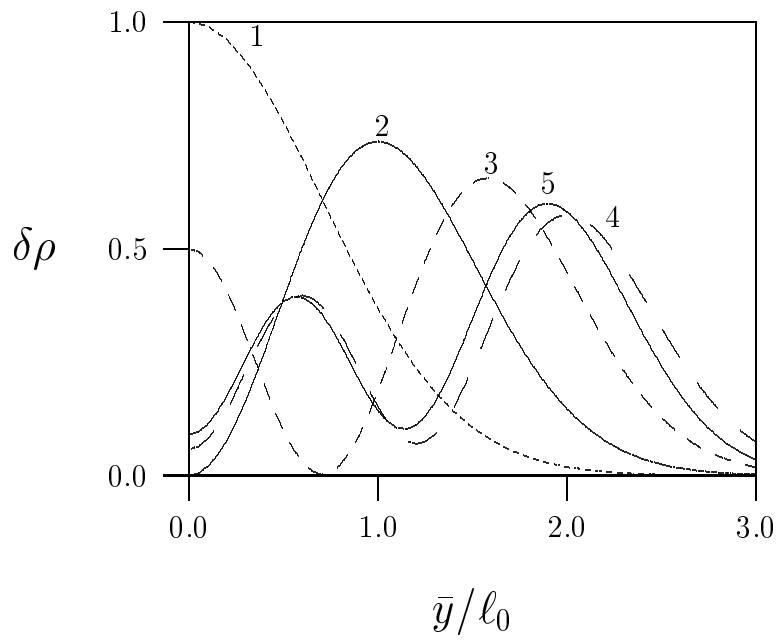


Fig. 1, Balev *et al.*

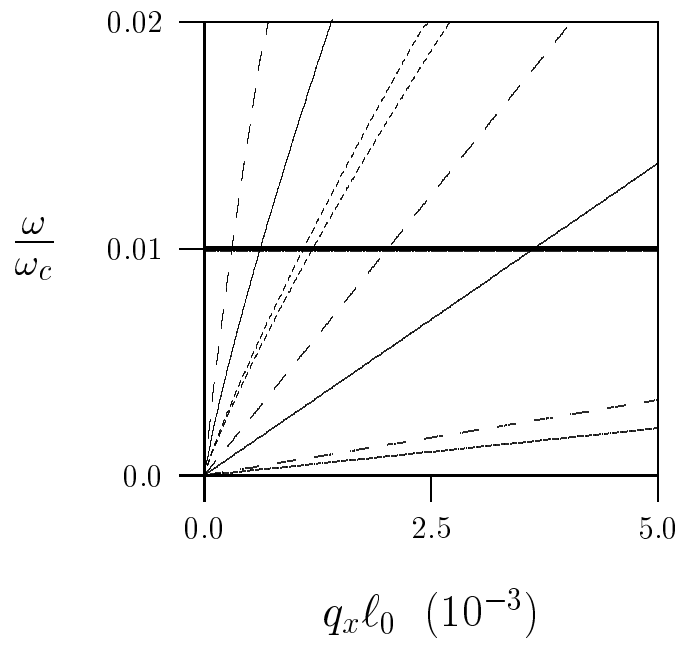


Fig. 3, Balev *et al.*